Synthesis and characterization of alumina fibers using solution blow spinning

(Síntese e caracterização de fibras de alumina por fiação por sopro em solução)

M. F. Mota[1]*, A. M. C. Santos[1], R. M. C. Farias[1], G. A. Neves[1], R. R. Menezes[1]
[1]Federal University of Campina Grande, Academic Unit of Materials Engineering, Materials Technology Laboratory, R. Aprígio Veloso 882, Campina Grande, PB, Brazil

Abstract

This work shows the successful production of alumina nanofibers after thermal treatment of solution blow spun hybrid fibers. These nanofibers were converted into γ-Al_2O_3 and α-Al_2O_3 after the thermal treatment in air between 500 to 1200 °C. The X-ray diffraction patterns presented all the characteristics of the γ and α phases of alumina. In addition, the scanning electron micrographs showed alumina nanofiber diameters varying between 200 and 270 nm for different temperatures. The results demonstrated that the solution blowing spinning method is efficient to produce alumina nanofibers.
Keywords: alumina, nanofibers, solution blow spinning.

Resumo

Esse trabalho mostra a produção de nanofibras de alumina após tratamento térmico de fibras híbridas preparadas por fiação por sopro em solução. Essas nanofibras foram convertidas em γ-Al_2O_3 e α-Al_2O_3 após tratamento térmico ao ar entre 500 e 1200 °C. Os padrões de difração de raios X apresentaram todas as características das fases alumina γ e α. Além disso, as micrografias eletrônicas de varredura mostraram que os diâmetros das nanofibras de alumina variaram entre 200 e 270 nm para diferentes temperaturas. Os resultados demonstraram que o método de fiação por sopro em solução é eficiente para produzir nanofibras de alumina.
***Palavra-chave**: alumina, nanofibras, fiação por sopro em solução.*

INTRODUCTION

Ceramic fibers have been studied in academic researches due to their commercial applications, such as catalysis, adsorbents, solar and fuel cells, sensors, filtration membranes, and tissue engineering [1]. Among the target spun materials, alumina (Al_2O_3) has received great attention once it is an important engineering material with high strength and elastic modulus, chemical stability and low thermal conductivity [2]. Alumina has several polymorphs namely α, γ, θ, η, δ, χ, κ, and β-Al_2O_3 and the alpha phase is the most thermodynamically stable form [3, 4]. The metastable forms also find application in anti-oxidative protective covers, membranes, catalysts, and catalysts supports [5].

Electrospinning (ES) is by far the most used top-down method for the production of ceramic nanofibers [6-8]. ES uses high electric fields (posing operational risks) to spin a precursor solution into hybrid fibers, followed by thermal treatments for removal of the organic component and ceramic formation. An emerging alternative method without ES drawbacks is the solution blow spinning (SBS) [9, 10]. In turn, SBS uses a high-speed gas stream as a driving force to spin the precursor solution into fibers making use of a simple set of concentric nozzles [11-13]. The fibers are rapidly processed and collected into different architectures such as fibrous membranes or cotton-wool-like structures [13], giving to SBS high benefit-to-cost ratio as compared to ES [12]. Most works on alumina fiber production have made use of ES as a spinning method. The SBS method was successfully used to produce alumina microfibers [14]. A comparative study between electro-blow spinning (EBS, junction of ES and SBS) and SBS was carried out and, as a result, microfibers were obtained with a diameter of 2.75 μm for EBS method and 4.12 μm for SBS method [15]. More recently, silica doped alumina microfibers were produced by EBS and the doping agent was found to likely act as a crystal growth inhibitor, positively impacting on the stability of polymorphs [16].

In this work, alumina nanofibers were produced from a precursor solution with aluminum nitrate nonahydrate using the solution blowing spinning technique. These nanofibers were calcined in air at temperatures ranging from 500 to 1200 °C to investigate the different polymorphic metastable forms of the structure, and the efficiency of the SBS method to obtain one-dimensional materials.

MATERIALS AND METHODS

Materials: aluminum nitrate nonahydrate (Sigma-Aldrich, Brazil) and polyvinylpyrrolidone (PVP, M_w ~1300000 g/mol, amorphous) were used as inorganic and

* https://orcid.org/0000-0002-7979-7272

organic precursors to form hybrid fibers. Ethanol (EtOH, 99.5%, Synth, Brazil) and distilled water were used as solvents for preparation of the solutions.

Fiber spinning: the precursor solution was prepared by dissolving aluminum nitrate nonahydrate (2.206 g) in a 2:1 ethanol/water mixture at constant stirring for 1 h. Later, 10 wt% of PVP was slowly added to the solution as a spinning agent and mixed for another hour. The final solution was transferred to a plastic syringe and then injected at 6.6 mL/h into the SBS inner nozzle, as shown in Fig. 1. The air pressure flowing through the external nozzle was set at 0.34 MPa. Fibers were spun across a tubular furnace at 300 °C to help solvent evaporation. The fibers were coll ected on a static collector placed in a chamber at 80 °C. The as-spun fibers were further calcined at different annealing temperatures from 500 to 1200 °C for 2 h.

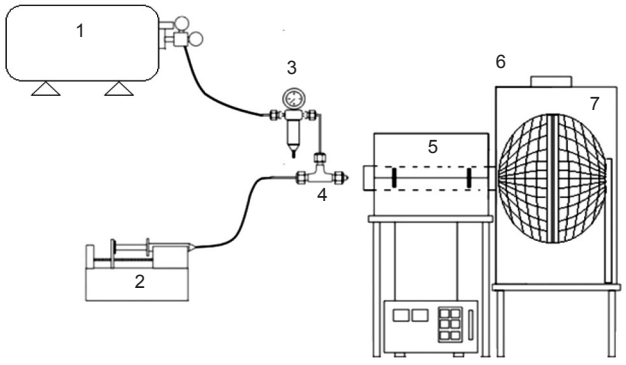

Figure 1: Schematic of SBS set-up: 1) air compressor; 2) injection pump; 3) pressure gauge; 4) concentric nozzles; 5) tubular furnace; 6) heated chamber; and 7) static collector.
[Figura 1: Esquema do conjunto de fiação por sopro em solução: 1) compressor de ar; 2) bomba de injeção; 3) manômetro; 4) bocais concêntricos; 5) forno tubular; 6) câmara aquecida; e 7) coletor estático.]

Fiber characterization: the fiber morphology was assessed by scanning electron microscopy (SEM, SSX-550, Shimadzu, Japan) of previously gold sputtered specimens. The fiber diameter was measured using the ImageJ software (National Institute of Health, USA) taking at least 50 individual fibers across two different sites. The thermogravimetric behavior of the as-spun fibers was simultaneously recorded with the differential thermal analysis in a thermal analyzer (DTG-60H, Shimadzu, Japan). The samples were heated from 25 to 1200 °C in an oxidizing atmosphere (synthetic air, 21% O_2+79% N_2) at a heating rate of 5 °C/min. The crystalline structure of the calcined fibers was evaluated by X-ray diffraction (XRD-6000, Shimadzu, Japan) with a Ni-filtered CuKα radiation source (λ=1.5418 Å) at 40 kV, 30 mA, 0.02 °.min^{-1} from 20° to 80° 2θ.

RESULTS AND DISCUSSION

Fiber morphology: since the morphological aspect of post-calcined fibers was quite similar, no matter the annealing temperature used, a unique SEM micrograph, typical of alumina nanofibers calcined at 500, 700 and 900 °C, is shown in Fig. 2. Nanofibers of circular cross-section and having smooth surface were successfully produced. The presence of bead-shaped structures was observed and this fact was ascribed to instabilities arising from the solution injection during the fiber processing. The average fiber diameter and diameter distribution, shown in Fig. 2, were in accordance with data from fibers obtained using ES as a spinning technique [17]. Curiously, the fiber average diameters were quite similar regardless of the annealing temperature applied, presented in Table I (216±77 and 250±72 nm for 500 and 1200 °C, respectively).

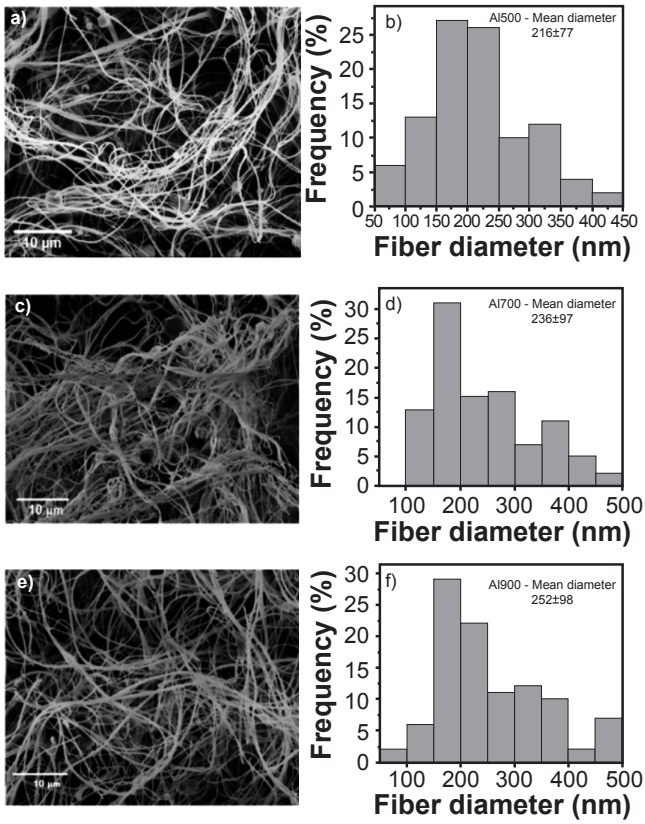

Figure 2: SEM micrograghs of alumina nanofibers calcined at: a) 500 °C; c) 700 °C; e) 900 °C; and diameter distribution of fibers calcined at: b) 500 °C; d) 700 °C; and f) 900 °C.
[Figura 2: Micrografias de MEV de nanofibras de alumina calcinadas a: a) 500 °C; c) 700 °C; e) 900 °C; e distribuição de diâmetro de fibras calcinadas a: b) 500 °C; d) 700 °C; e f) 900 °C.]

Thermal analysis: Fig. 3 shows the thermogravimetric (TG) and differential thermal analysis (DTA) curves of as-spun alumina nanofibers. Endothermic events corresponding to a mass loss of about 17% was seen in the temperature region extending to ca. 118 °C. These events were ascribed to the vaporization of physically absorbed water and the removal of the solvent residue of spun hybrid fibers. From 220 °C, the water present in the aluminum nitrate structure was removed. Another mass loss of 74% occurred between 220 and 430 °C, which was mainly related to the decomposition of PVP organic phase and its carbonic residues present in the sample. The weight loss observed at

Table I - Mean diameter ± standard deviation of alumina nanofibers calcined between 500 to 1200 °C.
[Tabela I - Diâmetro médio ± desvio padrão das nanofibras de alumina calcinadas entre 500 e 1200 °C.]

Temperature (°C)	500	600	700	800	900	1000	1100	1200
Diameter (nm)	216±77	259±97	236±97	265±144	252±98	250±107	250±72	247±79

around 500 °C and the exothermic peak at this temperature were associated with the combustion of PVP carbonaceous residue. PVP degraded basically in two stages: one between 220 and 430 °C related with the degradation of the side chain of PVP, and other between 450 and 550 °C resulted from the oxidation and decomposition of polymer residues [18-23]. Moreover, above 550 °C mass losses did not occur and only the polymorphic alumina transformations took place. Although the PVP was removed during thermal treatment, a proper PVP content is essential for efficient calcination when producing alumina nanofibers [24, 25].

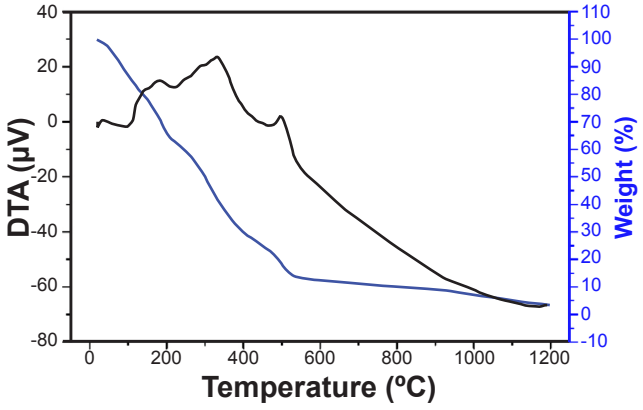

Figure 3: TG and DTA curves of the as-spun nanofiber.
[Figura 3: Curvas de TG e DTA de nanofibra como fiada.]

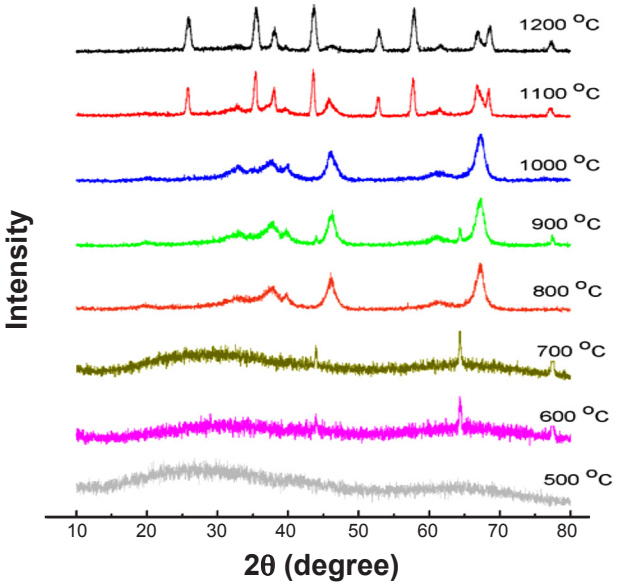

Figure 4: X-ray diffraction patterns of alumina nanofibers calcined at different temperatures.
[Figura 4: Padrões de difração de raios X das nanofibras de alumina calcinadas em diferentes temperaturas.]

XRD analysis: the phase evolution of alumina fibers was followed at different annealing temperatures, namely from 500 to 1200 °C. The XRD patterns are shown in Fig. 4. At 500 °C, a typical amorphous material pattern was found. As the annealing temperature increased from 600 to 1000 °C, characteristic peaks of γ-Al_2O_3 metastable phase appeared. The XRD patterns also showed the coexistence of γ and α-Al_2O_3 at 1100 °C indicating that the phase transition occurred between 1000 and 1100 °C, similarly to that found in [15]. Nanofibers of γ-Al_2O_3 obtained in the range of 800 to 1000 °C showed three characteristic peaks at 2θ 44.1°, 64.3°, and 77.4°. These peaks became more intense at higher temperatures indicating high crystalline phase. At 1200 °C, the peaks observed for 2θ values of 25.6°, 35.4°, 38.0°, 43.6°, 52.6°, and 57.7° suggested the phase transition of most part of γ-Al_2O_3 to the most stable phase α-Al_2O_3 [26-28].

CONCLUSIONS

Alumina nanofibers were successfully produced using solution blow spinning (SBS). The SEM micrographs revealed the presence of fibers with diameters ranging from 200 to 270 nm, though some bead structures were present. The annealing temperature did not affect fiber diameter. XRD patterns revealed the formation of γ-Al_2O_3 and α-Al_2O_3 at temperatures next to 1100 °C. The thermal treatment analysis presented mass losses that occurred during the process of calcination. We also found that the fiber diameter and distribution presented a homogeneity that indicated the reproducibility of the SBS method. The results of the present study demonstrated that the SBS is suitable for obtaining alumina nanofibers at a low cost.

ACKNOWLEDGMENTS

This work was supported by CAPES and CNPq. The authors are also grateful to Science and Material Engineering Graduate Program from the Federal University of Campina Grande.

REFERENCES

[1] R. Ramaseshan, S. Sundarrajan, R. Jose, S. Ramakrishna, J. Appl. Phys. **102**, 11 (2007) 7.
[2] W. Kang, B. Cheng, Q. Li, X. Zhuang, Y. Ren, Text. Res. J. **81**, 2 (2011) 148.
[3] H. Yang, M. Liu, J. Ouyang, Appl. Clay Sci. **47**, 3 (2010) 438.
[4] Y. Men, H. Gnaser, C. Ziegler, Anal. Bioanal. Chem. **375**, 7 (2003) 912.

[5] W.E. Lee, M. Rainforth, *Ceramic microstructures: property control by processing*, Springer, Netherlands (1994).
[6] M. Vahtrus, M. Umalas, B. Polyakov, L. Dorogin, R. Saar, M. Tamme, S. Vlassov, Mater. Charact. **107** (2015) 119.
[7] P.C. Yu, R.J. Yang, Y.Y. Tsai, W. Sigmund, F.S. Yen, J. Eur. Ceram. Soc. **31**, 5 (2011) 723.
[8] Z. Zhao, X. Shen, H. Yao, J. Wang, J. Chen, Z. Li, J. Sol-Gel Sci. Technol. **70**, 1 (2014) 72.
[9] R.M. da Costa Farias, R.R. Menezes, J.E. Oliveira, E.S. de Medeiros, Mater. Lett. **149** (2015) 47.
[10] B. Cheng, X. Tao, L. Shi, G. Yan, X. Zhuang, Ceram. Int. **40**, 9 (2014) 15013.
[11] E.S. Medeiros, G.M. Glenn, A.P. Klamczynski, W.J. Orts, L.H. Mattoso, J. Appl. Polym. Sci. **113**, 4 (2009) 2322.
[12] J.E. Oliveira, E.A. Moraes, R.G. Costa, A.S. Afonso, L.H. Mattoso, W.J. Orts, E.S. Medeiros, J. Appl. Polym. Sci. **122**, 5 (2011) 3396.
[13] A.M.C. Santos, M.F. Mota, R.S. Leite, G.A. Neves, E.S. Medeiros, R.R. Menezes, Ceram. Int. **44**, 2 (2018) 1681.
[14] L. Li, W. Kang, X. Zhuang, J. Shi, Y. Zhao, B. Cheng, Mater. Lett. **160** (2015) 533.
[15] L. Li, W. Kang, Y. Zhao, Y. Li, J. Shi, B. Cheng, Ceram. Int. **41**, 1 (2015) 409.
[16] X.H. Zhou, J.G. Ju, Z.H. Li, M.L. Zhang, N.P. Deng, B.W. Cheng, W.M. Kang, Ceram. Int. **43**, 13 (2017) 9729.
[17] P. Liu, Y. Zhu, J. Ma, S. Yang, J. Gong, J. Xu, Colloids Surf. A **436** (2013) 489.
[18] X. Chen, F. Zhang, Q. Wang, X. Han, X. Li, J. Liu, F. Qu, Dalton Trans. **44**, 7 (2015) 3034.
[19] M.M. Abualrejal, H. Zou, J. Chen, Y. Song, Y. Sheng, Adv. Nanopart. **6**, 2 (2017) 33.
[20] J. Liu, W. Li, L. Zhu, C. Li, F. Qu, W. Guo, S. Ruan, J. Nanosci. Nanotechnol. **14**, 5 (2014) 3653.
[21] A. Mahapatra, B.G. Mishra, G. Hota, Ceram. Int. **37**, 7 (2011) 2329.
[22] J. Chen, Y. Sheng, X. Zhou, M.M. Abualrejal, M. Chang, Z. Shi, H. Zou, RSC Adv. **6**, 20 (2016) 16452.
[23] O. Elishav, V. Beilin, O. Rozent, G.E. Shter, G.S. Grader, J. Polym. Sci. B **56**, 3 (2018) 248.
[24] X. Song, W. Liu, J. Wang, S. Xu, B. Liu, J. Liu, Y. Ma, Ceram. Int. **43**, 13 (2017) 9831.
[25] J.H. Kim, S.J. Yoo, D.H. Kwak, H.J. Jung, T.Y. Kim, K.H. Park, J.W. Lee, Nanoscale Res. Lett. **9**, 1 (2014) 44.
[26] M. Aghayan, N. Voltsihhin, M.A. Rodríguez, F. Rubio-Marcos, M. Dong, I. Hussainova, Ceram. Int. **40**, 8 (2014) 12603.
[27] X. Tang, Y. Yu, Ceram. Int. **41**, 8 (2015) 9232.
[28] Y. Wang, W. Li, X. Jiao, D. Chen, J. Mater. Chem. A **1**, 36 (2013) 10720.
(Rec. 17/05/2018, Rev. 26/09/2018, 08/11/2018, Ac. 09/11/2018)